Summary: Properties of a series of hyperbranched polyfluorenes were investigated. Increasing the benzene ''crosspoint'' density blue-shifts the absorption and PL since the crosspoints interrupt π-electron conjugation, decreasing conjugation length, and thus increasing chromophore band gap. The relative intensity of $S_{10} \rightarrow S_{00}$ transition in PL increases with crosspoint density increase, indicating that the energy and the energy distribution of vibronic transitions were controlled by hyperbranch structure. When the polymer solution is cooled down, the lattice vibration is reduced and the effective conjugation length (coherence length for electron wavefunction) is increased, thus causing bathochromic shift in absorption and PL. These polymers do not favor excimer formation in solution due to their remarkable rigidity and extra-large molecular size. With increase in crosspoint density, LED color changed from green to violet. In double-layer LEDs, PPV not only improves hole injection/transport but also contributes to device emission through its bulk emission and interfacial emission as a result of interfacial energy transfer. Higher electrical field favors interfacial energy transfer probably by facilitating hole–electron recombination and by encouraging the excitons formed in polyfluorene layer to migrate to the interface and to further diffuse into PPV layer. The polymer with more crosspoints shows higher EL efficiency. The crosspoints interrupt π-electron conjugation, isolate excitons and inhibit intrachain exciton annihilation. They can also increase rigidity of the macromolecular backbone, and the large spatial hindrance of these macromolecules makes the molecular packing very difficult, thus decreasing interchain exciton annihilation. All these structural features help to increase exciton lifetime and improve LED performance.

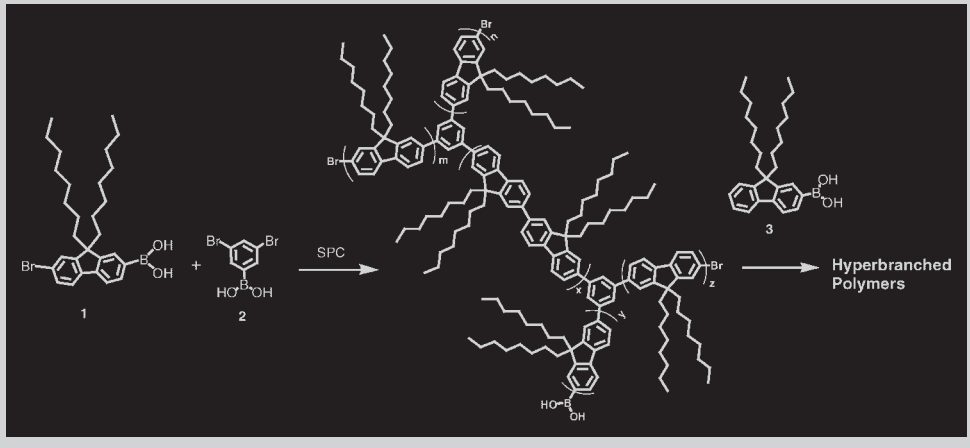

Synthesis of the hyperbranched polyfluorenes.

Photophysical and Electroluminescent Properties of Hyperbranched Polyfluorenes

Liming Ding,[1,2] *Zhishan Bo,*[3] *Qinghui Chu,*[4] *Jing Li,*[3] *Liming Dai,*[2] *Yi Pang,*[4] *Frank E. Karasz,*[1] *Michael F. Durstock*[5]

[1] Department of Polymer Science & Engineering, University of Massachusetts, Amherst, Massachusetts 01003, USA
E-mail: Ding@polysci.umass.edu
[2] Department of Materials Engineering, University of Dayton, Dayton, Ohio 45469, USA
[3] State Key Laboratory of Polymer Physics & Chemistry, Institute of Chemistry, Chinese Academy of Sciences, Beijing 100080, P. R. China
[4] Department of Chemistry, University of Akron, Akron, Ohio 44325, USA
[5] Polymer Branch, Air Force Research Laboratory, Wright-Patterson Air Force Base, Ohio 45433, USA

Received: February 4, 2006; Revised: March 15, 2006; Accepted: March 15, 2006; DOI: 10.1002/macp.200600055

Keywords: electroluminescence; energy transfer; exciton confinement; density; hyperbranched polyfluorene; photoluminescence; structures

Introduction

The discovery of electroluminescence (EL) in poly(*p*-phenylene vinylene)[1] has stimulated a large number of research on conjugated polymers with the aim of chemically tuning the emission color, adjusting the charge transport properties, improving device quantum efficiency, improving film-forming capability, and developing new optoelectronic applications.[2–6] Star-branched or hyperbranched conjugated polymers have received considerable attention for device application due to their synthetic simplicity, good solubility, high fluorescence quantum yields, the ability to form amorphous films of high quality, and good thermal stability.[7–17] The hyperbranched molecular structure favors exciton confinement and decreases intrachain and interchain exciton annihilation thereby improving EL efficiency significantly. Fomina and Salcedo synthesized a conjugated hyperbranched polymer. Their theoretical calculations using the AM1 method indicated that the conjugation in the polymer is partially disrupted by the twisting of the benzene rings.[18] Moore and coworkers observed discrete exciton localization on isolated absorbing units within the backbone of a phenylacetylene dendrimer.[19] One-pot Suzuki polycondensation (SPC) of the AB_2 monomers carrying flexible alkyl chains produced high-molecular weight fluorene-triphenylamine alternating hyperbranched copolymers, which are fully soluble in common organic solvents.[8c] In this paper, the photophysical and electroluminescent properties of a series of light-emitting hyperbranched polyfluorenes **1**–**3**[8a] (see Scheme 1) were reported. The effect of molecular structure, temperature, and chromophore aggregation on solution absorption and photoluminescence was studied. Double-layer LEDs were fabricated, and the interfacial energy transfer phenomenon in devices ITO/PPV/polymer/Ca was discussed.

Experimental Part

The synthesis and characterization of hyperbranched polymers **1**–**3** have been reported and **1**–**3** correspond to **P5**, **P15**, and **P40** in ref.[8a], respectively. PPV/ITO substrates were obtained by spin-casting methanol solution of the precursor polymer[1] on to ITO glass (OFC Co.) and then thermally converting to PPV under flowing argon at 250 °C for 2.5 h. PEDOT/PSS (Bayer Co.) was spin-cast directly on to ITO glass. The polymer solutions (10 mg/ml in chloroform) were filtered through 0.2 μm Millex-FGS Filters (Millipore Co.), and were spin-cast on to PPV/ITO substrates or dried PEDOT/ITO substrates under a nitrogen atmosphere. Calcium electrodes of 400 nm thickness were evaporated on to the polymer films at about 10^{-7} Torr, followed by a protective coating of aluminum. The electroluminescent properties of the devices sealed in argon were measured as described elsewhere.[20] PL spectra were recorded on a Perkin Elmer LS55 Luminescence Spectrometer. UV-Vis absorption spectra were recorded on a HITACHI U-3010 UV-Vis spectrophotometer. Thickness of the polymer films was measured by using a Dektak 3030 Surface Profiler. A Hewlett-Packard 8453 diode array spectrophotometer and a PTI steady-state fluorometer were also used for photophysical measurements. The low-temperature spectra were taken by using a low-temperature Dewar vessel. Electrochemical measurements were performed on PARSTAT 2263 by using the standard three-electrode cell, which consisted of a platinum working electrode, a platinum gauze counterelectrode, and an Ag/AgCl reference electrode. Measurements were carried out in an electrolyte solution of 0.1 M tetrabutylammonium tetrafluoroborate dissolved in dry, degassed acetonitrile (distilled over CaH_2). Typical cyclic voltammograms were recorded at a scan rate of 50 $mV \cdot s^{-1}$ for a thin polymer film, which was deposited on the platinum working electrode under argon.

Results and Discussion

Absorption and Emission of Solution and Film

The absorption spectra of solutions and films of polymers **1**–**3** are shown in Figure 1. The respective absorption peak

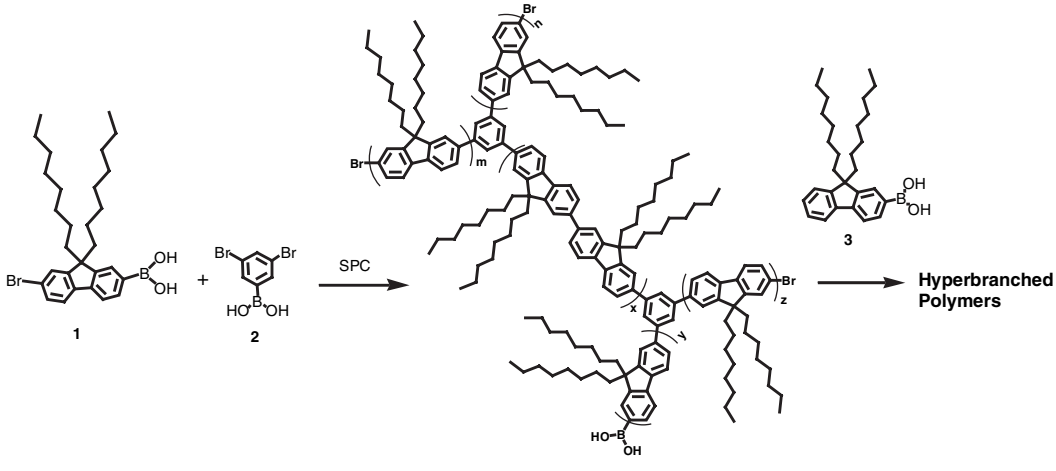

Scheme 1. Synthesis of the hyperbranched polyfluorenes.

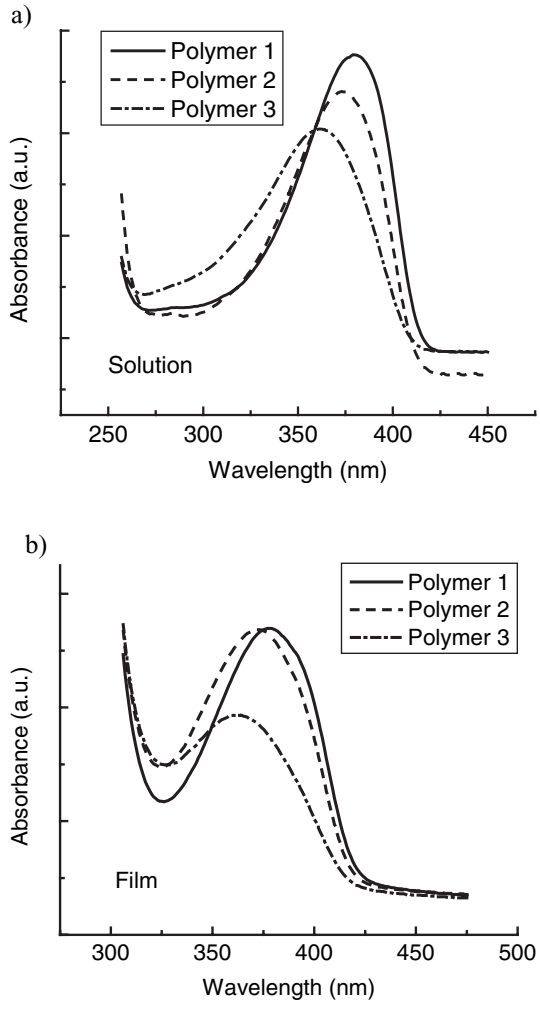

Figure 1. Absorption spectra for polymers **1**, **2**, and **3**.

wavelengths for the solutions of **1**–**3** are 379, 373, and 362 nm (Table 1). This indicates that increasing the content of 1,3,5-substituted benzene ''crosspoints'' blue-shifts the absorption spectra as the 1,3,5-substituted benzene ring interrupts conjugation, decreasing conjugation length, and thus increasing the chromophore band gap. Similar phenomena were observed in the films. The absorption peak wavelengths for films of **1**–**3** are 378, 372, and 362 nm, respectively. The PL spectra of solutions and films of polymers **1**–**3** are shown in Figure 2. The emission peak wavelengths of the solutions **1**–**3** are 417 (440), 416 (438), and 415 (437) nm, respectively. The numbers and the numbers in the parentheses correspond to the $S_{10} \rightarrow S_{00}$ and $S_{10} \rightarrow S_{01}$ vibronic transitions, respectively. It is observed that the relative intensity of the $S_{10} \rightarrow S_{01}$ band decreases with increase in benzene crosspoint density. The PL spectra for polymers **1**–**3** in solid state also show fine vibronic structures. The peak wavelengths are 444, 428, and 425 nm, respectively. In addition to the blue-shift in the PL, the relative intensity of the $S_{10} \rightarrow S_{00}$ transition increases with

Table 1. Photophysical properties of the polymers.

Polymer	λ_{max}^{Abs} / nm		$\lambda_{max}^{PL\ a,b)}$ / nm	
	Solution	Film	Solution	Film
1	379	378	**417**, 440	431, **444**, 478(sh)
2	373	372	**416**, 438	**428**, 444, 476(sh)
3	362	362	**415**, 437(sh)	**425**, 442, 475(sh)

[a] Bold data indicates the most intense peak.
[b] Excitation wavelength 300 nm.

increase in the benzene crosspoint density, indicating that the energy and energy distribution of the vibronic transitions depend on the hyperbranch structure of these polymers. Compared with the solution PL, the film photoluminescence shows a 10–27 nm red shift, indicating the chromophore–chromophore interaction in the solid state.

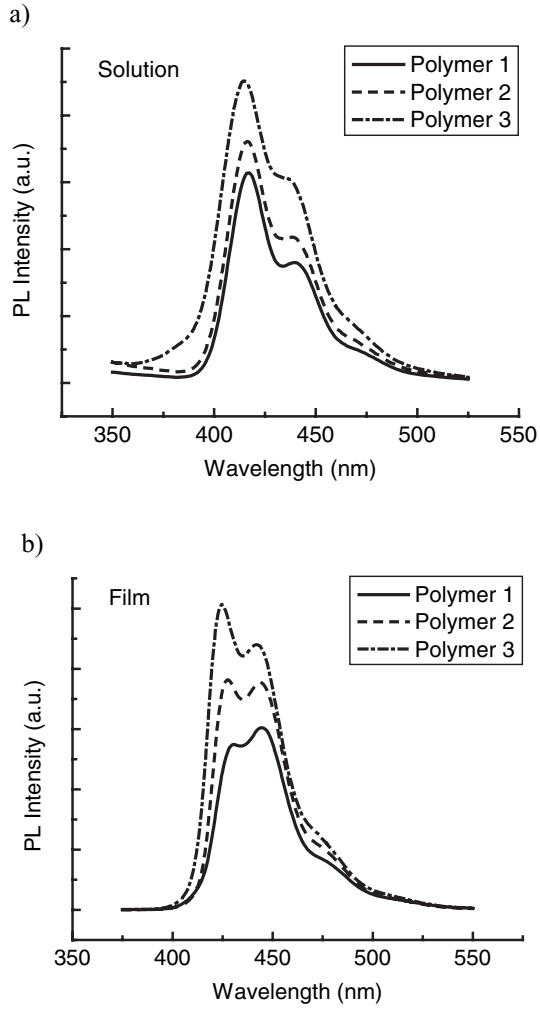

Figure 2. PL spectra for polymers **1**, **2**, and **3**.

Low-Temperature Photophysical Properties

The low-temperature absorption and emission spectra of polymer **2** in THF are shown in Figure 3. As the polymer solution was cooled down from 20 to −108 °C, the absorption peak made a red-shift of 6 nm. The low-temperature PL spectrum exhibited a similar spectral red-shift, showing two peaks (420 and 438 nm) and two shoulders (469 and 504 nm). This red-shift in absorption and emission at low temperature is similar to that observed previously by Rothberg and co-workers[21] and Heeger and co-workers.[22] When the conjugated polymer solution is cooled down, the lattice vibration is reduced and the effective conjugation length (coherence length for the electron wavefunction) is increased,[21] thus causing a red-shift. For low-temperature PL spectrum, apart from the red-shift, the relative intensities of $S_{10} \rightarrow S_{01}$, $S_{10} \rightarrow S_{02}$, $S_{10} \rightarrow S_{03}$ vibronic bands increased evidently. This might result from the excimer emission at low temperature. It is suggested that the low-temperature PL spectrum is the sum of an excitonic spectrum as that at room temperature and the excimer emission.[23] For polymer **2** solution, the vibrational spacings between $S_{10} \rightarrow S_{00}$ and $S_{10} \rightarrow S_{01}$ bands are 1 207 and 979 cm^{-1} at 20 and −108 °C, respectively. At low temperature, the vibrational spacing decreases. This phenomenon is different from a previous report on MEH-PPV film,[21] which might result from the difference in polymer structure, state (solution or film), and temperature.

Chromophore Aggregation

Figure 4 shows the PL spectra of polymer **2** in chloroform (3 ml) upon addition of the non-solvent methanol. With the increase in methanol content, the PL spectra show red-shift, which originates from intermolecular excimer formation. The red-shift in PL resulting from chromophore aggregation in solvent/non-solvent mixture is similar to previous work.[24,25] However, the spectral red-shift and shape change in this case are not so remarkable as that observed in a solution of linear conjugated polymers. This might be due to the rigidity and large molecular size of the hyperbranched polyfluorene which does not favor excimer formation.

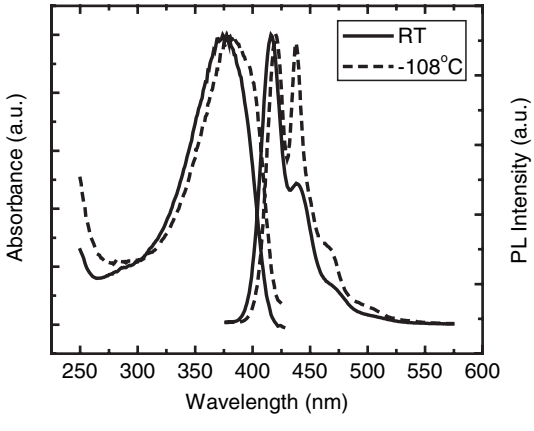

Figure 3. Normalized absorption and PL spectra of polymer **2** in THF at room temperature and −108 °C, respectively.

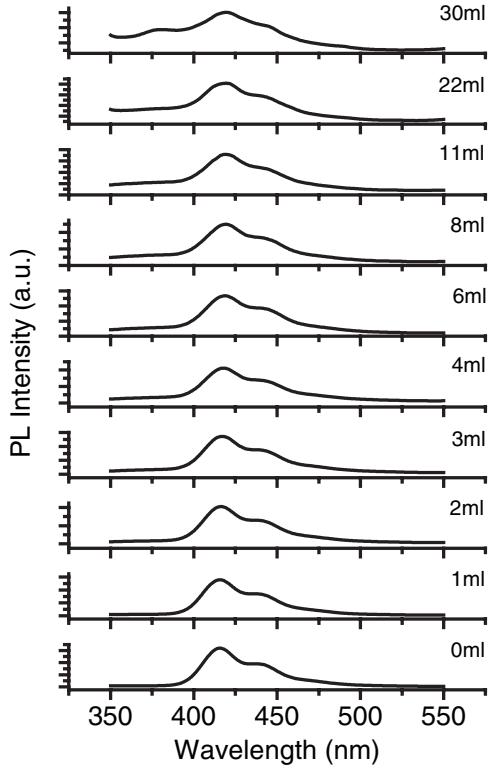

Figure 4. PL spectra of polymer **2** in chloroform (3 ml) upon addition of non-solvent methanol.

Electrochemical Properties

The electrochemical behavior of the polymers was investigated by cyclic voltammetry (CV). The onset potentials for oxidation of polymers **1**–**3** were observed to be 1.41, 1.43, and 1.47 V, respectively (Table 2). By using the empirical relations,[26] the ionization potentials (IP), i.e., the HOMO levels, of polymers **1**–**3** were estimated to be −5.81, −5.83, and −5.87 eV, respectively. The LUMO

Table 2. Electrochemical results of the polymers.

Polymer	Bandgap[a)]	E_{ox}[b)]	HOMO	LUMO
	eV	V	eV	eV
1	2.99	1.41	−5.81	−2.82
2	3.01	1.43	−5.83	−2.82
3	3.03	1.47	−5.87	−2.84

[a)] Obtained from the absorption spectra.
[b)] Onset oxidation potentials versus Ag/AgCl reference electrode.

energy levels of **1**–**3**, which were calculated from the respective HOMO energy levels and the optical bandgaps, were −2.82, −2.82, and −2.84 eV, respectively. With increase of 1,3,5-substituted benzene crosspoints, polymer LUMO energy level can be lowered. Generally, the band gap value of conjugated polymers obtained by electrochemical method are larger than that from absorption spectra,[27] which might result from the interface barrier for charge injection in the electrochemical process as suggested by Chen et al.[27a] and Yamamoto and co-workers.[27b] So, it should be noted here that the above method used to estimate the LUMO energy levels is not quite exact.

Double-Layer LEDs and Interfacial Energy Transfer

To improve LED performance and investigate the interfacial energy transfer in double-layer LEDs, the devices were fabricated with the configurations of ITO/PEDOT/polymer/Ca and ITO/PPV/polymer/Ca. The PEDOT and PPV layers were used to improve hole injection and transport from the anode. The EL results are summarized in Table 3. Device ITO/PEDOT/**1**/Ca shows three emission peaks (426, 450, and 482 nm) and one shoulder at 512 nm (Figure 5), corresponding to $S_{10} \rightarrow S_{00}$, $S_{10} \rightarrow S_{01}$, $S_{10} \rightarrow S_{02}$, and $S_{10} \rightarrow S_{03}$ vibronic transitions, respectively. Comparing with the solid state PL spectrum of polymer **1**, it can be seen that the three bands shown in the PL are also displayed in EL spectrum though their relative intensities differ. The EL spectrum shows an additional $S_{10} \rightarrow S_{03}$ vibronic band and broadens evidently. The different exciton formation processes (electron-hole recombination vs. photoexcitation) lead to emissions with different energy and vibronic fine structures. Excimer emission may also contribute to the remarkable EL spectral broadening. LED using polymer **2** shows four emission bands at 421, 443, 474, and 507 nm, respectively. The $S_{10} \rightarrow S_{00}$ band is the strongest. The EL spectrum of polymer **3** is quite similar to its PL spectrum with peaks at 420 and 442 nm and a shoulder at 471 nm. From polymers **1** to **3**, with increase in benzene crosspoint density, the EL spectra show continuous blue-shifts because of the decrease of the effective conjugation length, and LED emission color changed from green to violet. By chemically adjusting the crosspoint density of the hyperbranched conjugated polymers, the LED color tuning can be realized.

Table 3. EL properties of the polymers.

Polymer	ITO/PEDOT/polymer/Ca		
	λ_{max}^{EL} [a]	Turn-on voltage	QE_{ext} [b]
	nm	V	
1	426, 450, **482**, 512(sh)	3.5	1.39%
2	**421**, 443, 474, 507(sh)	4.5	1.74%
3	**420**, 442, 471(sh)	4.5	2.46%
Polymer	ITO/PPV/polymer/Ca		
	λ_{max}^{EL} [a]	Turn-on voltage	QE_{ext} [b]
	nm	V	
1	425, **451**, 507	11	0.21%
2	416, **440**, 469(sh), 504, 537(sh)	10	0.41%
3	424, **500**	19	1.06%

[a] Bold data indicates the most intense peak.
[b] Maximum external quantum efficiency.

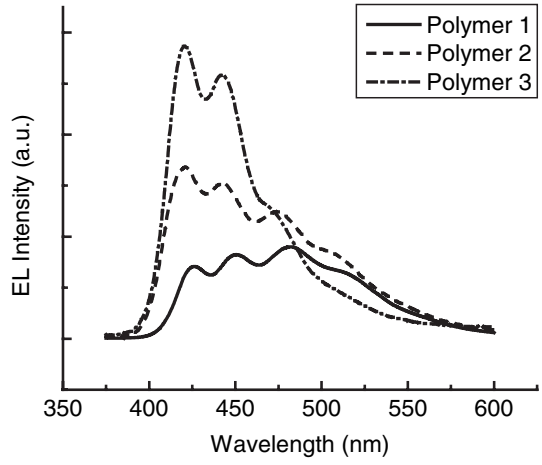

Figure 5. EL spectra for devices ITO/PEDOT/polymer/Ca.

As discovered in our previous work,[20] in double-layer LEDs, PPV as a hole-transporting material not only improves hole injection/transport but also contributes to the device emission in terms of its bulk emission and interfacial emission as a result of interlayer energy transfer. Two requirements for realizing efficient Förster energy transfer between two conjugated polymers are as follows: sufficient spectral overlap between the emission of the higher band-gap polymer and the absorption of the lower band-gap polymer, and a Förster interaction range of 3–4 nm.[28] In this study, the PL spectra of polymer **1**–**3** films overlap with the absorption spectrum of the PPV film almost completely as shown in Figure 6; therefore, substantial energy transfer between the layers of polymers **1**–**3** and the PPV layer at the interface is feasible. Figure 7 shows the EL spectra for the devices ITO/PPV/polymer/Ca and the EL spectrum of an ITO/PPV (31 nm)/Ca device shown for comparison. The device ITO/PPV/**1**/Ca emits blue-green light at 425, 451, and 507 nm. The 425 and 451 nm bands agree very well with the PL spectrum of a polymer **1** film, indicating that they come from the polymer **1** layer. Since the 507 nm band is quite different from the PPV feature emission, it can be regarded as a combination of the bulk PPV emission and the PPV/**1** interface emission.

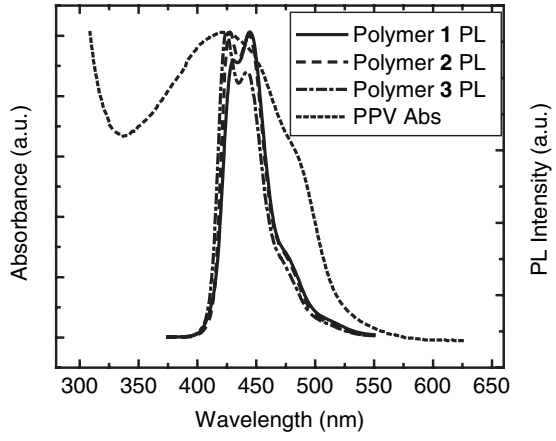

Figure 6. Spectral overlap between absorption of PPV film and emission from polymer **1**–**3** films.

The device ITO/PPV/**2**/Ca shows a blue-shifted EL spectrum with peaks at 416, 440, 469(sh), 504, 537(sh) nm. The blue-shift is due to the higher band gap of polymer **2**. Obviously the first three peaks originate from polymer **2** and the last two from PPV. Device ITO/PPV/**3**/Ca yields a strong emission at 500 nm which can be attributed to the high interfacial energy transfer between polymer **3** and the PPV layer. The minor band at 424 nm should originate from the polymer **3** layer. Comparing with the EL spectrum of pure PPV consisting of two bands at 500 and 529 nm, the emission resulting from interfacial energy transfer presents only the $S_{10} \rightarrow S_{00}$ transition of the PPV emission, indicating a substantial difference between the emission from the PPV/**3** interface and that from bulk PPV, which further supports the existence of interfacial energy transfer.

Voltage Dependence of EL Spectra

The voltage dependence of EL spectra is shown in Figure 8. For the device ITO/PEDOT/**2**/Ca, as the applied voltage increases from 7 to 9 V, the relative intensity of the high-energy vibronic transition $S_{10} \rightarrow S_{00}$ increases even though the vibronic fine structure of the spectrum does not change significantly. For the device ITO/PPV/**1**/Ca, as the applied voltage increases from 17 to 25 V, the emission bands from polymer **1** are relatively unchanged and only the $S_{10} \rightarrow S_{00}$ band shows a small blue-shift. But the emission at 503 nm originating from bulk PPV and the PPV/**1** interface increases evidently indicating that the higher applied electrical field favors interfacial Förster energy transfer probably by facilitating hole–electron recombination and by encouraging the excitons formed in hyperbranched polymer layer to migrate to the interface and to diffuse into the PPV layer.

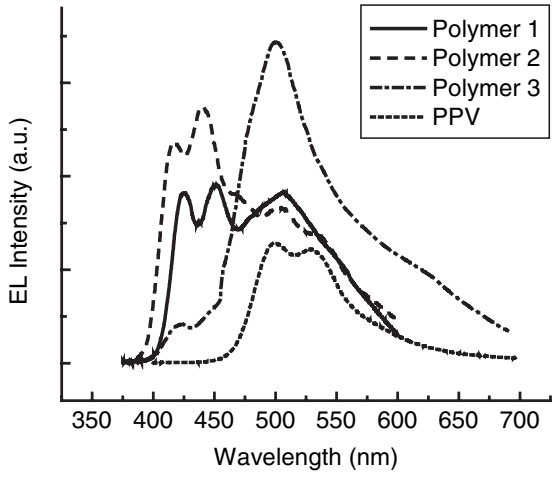

Figure 7. EL spectra for devices ITO/PPV/polymer/Ca. EL spectrum of device ITO/PPV/Ca was inset for comparison.

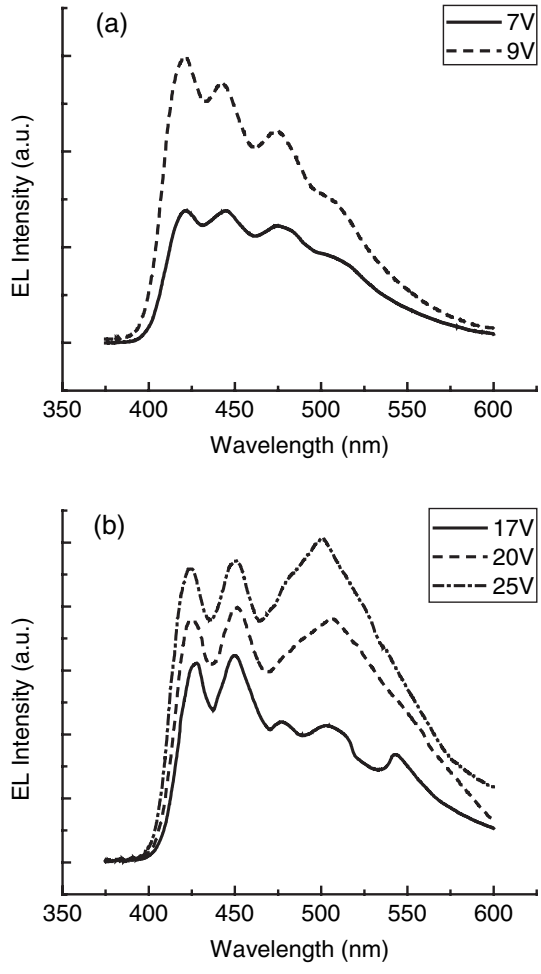

Figure 8. Voltage dependence of EL spectra for devices (a) ITO/PEDOT/**2**/Ca and (b) ITO/PPV/**1**/Ca.

Current–Voltage–Luminance Relationships

Current density versus voltage, and luminance versus voltage characteristics for the ITO/PEDOT/polymer/Ca and ITO/PPV/polymer/Ca devices are shown in Figure 9

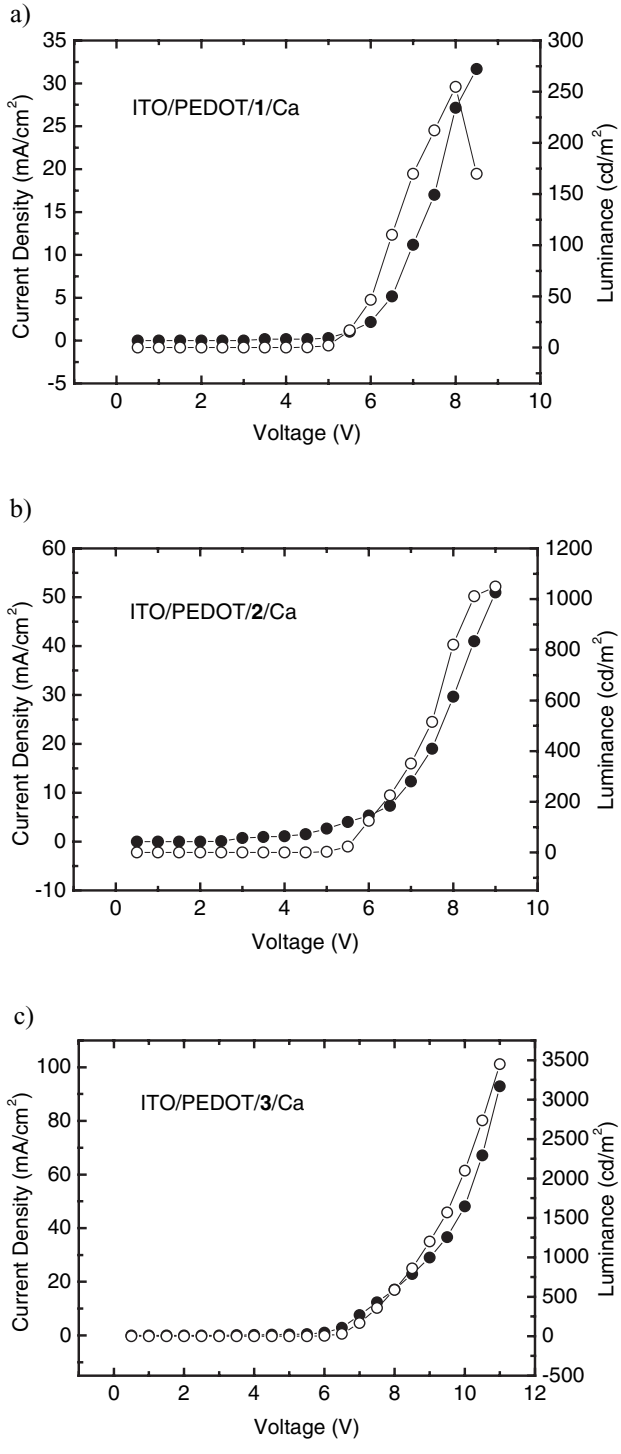

Figure 9. Current density (●) versus voltage and luminance (○) versus voltage characteristics for devices ITO/PEDOT/polymer/Ca.

and 10. PEDOT-containing LEDs for polymers **1**–**3** show turn-on voltages of 3.5, 4.5, and 4.5 V, respectively, and maximum external quantum efficiencies of 1.39, 1.74, and 2.46%, respectively. PPV-containing LEDs for polymers **1**–**3** show turn-on voltages of 11, 10, and 19 V, respectively, and maximum external quantum efficiencies of 0.21, 0.41, and 1.06%, respectively. Since the PEDOT workfunction (5.2 eV) is higher than that of PPV (5.0 eV),[29,30] the PEDOT layer is more effective in reducing the hole-injection barrier at the anode interface than the PPV layer,

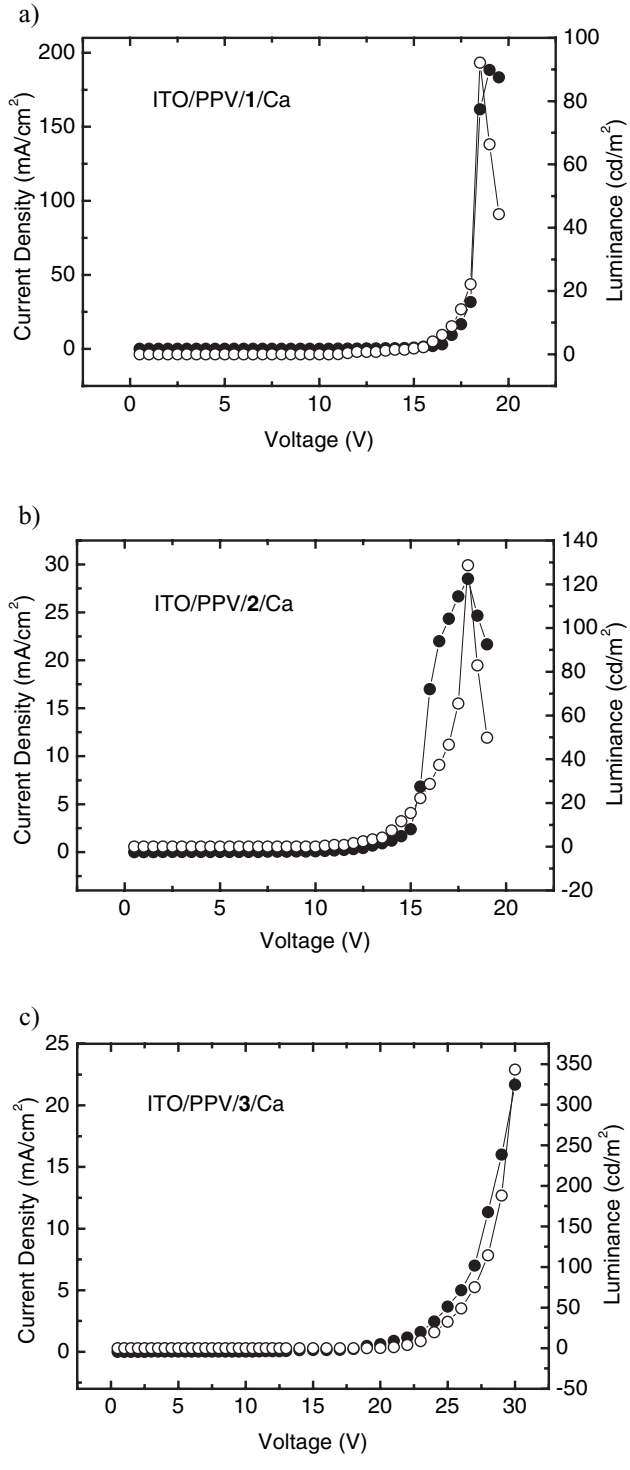

Figure 10. Current density (●) versus voltage and luminance (○) versus voltage characteristics for devices ITO/PPV/polymer/Ca.

thus PEDOT devices show much lower turn-on voltages. The built-in field of the LEDs fabricated with identical cathodes scale with the workfunctions of the different anodes,[29] so the higher the workfunction of the polymer anode, the higher the built-in field across the emitting layer, and the higher the EL efficiency. It is very interesting to note that the hyperbranched polyfluorene with higher density of the benzene crosspoint shows higher EL efficiency. The 1,3,5-substituted benzene ring can interrupt conjugation, isolate excitons, and inhibit intrachain exciton annihilation. The benzene ring can also increase the rigidity of the molecular backbone and the large spatial hindrance of these polymers lets the molecular packing more difficult, thus decreases interchain exciton annihilation. All these structural features can help to increase exciton lifetime and improve exciton radiative decay efficiency.

Conclusion

The photophysical and electroluminescent properties of a series of light-emitting hyperbranched polyfluorenes were systematically studied. The optical properties of these materials show significant dependence on the 1,3,5-substituted benzene crosspoint density. Increasing the content of benzene crosspoints blue-shifts the absorption and emission since the 1,3,5-substituted benzene ring interrupts π-electron conjugation, which decreases conjugation length, and thus increases the chromophore bandgap. With increase in crosspoint density, the emission color of the PEDOT-containing LEDs shift from green to violet. The PPV-containing LEDs emit blue and blue-green light. The hyperbranched conjugated macromolecules with more benzene crosspoints show higher EL efficiency due to the effective exciton confinement and the reduction of intrachain or interchain exciton annihilation. It was found that higher applied electrical field enhances interfacial energy transfer. The very broad EL spectra of these hyperbranched macromolecules consisting of emission bands of different color from violet to green may permit them to be used in the fabrication of white LEDs.

Acknowledgements: Financial support from *AFOSR* is acknowledged. L.D. would thank one of the referees for giving valuable comments on the energy level calculation.

[1] J. H. Burroughes, D. D. C. Bradley, A. R. Brown, R. N. Marks, K. Mackay, R. H. Friend, P. L. Burns, A. B. Holmes, *Nature* **1990**, *347*, 539.
[2] [2a] J. S. Wilson, M. J. Frampton, J. J. Michels, L. Sardone, G. Marletta, R. H. Friend, P. Samori, H. L. Anderson, F. Cacialli, *Adv. Mater.* **2005**, *17*, 2659; [2b] C. L. Donley, J. Zaumseil, J. W. Andreasen, M. M. Nielsen, H. Sirringhaus, R. H. Friend, J.-S. Kim, *J. Am. Chem. Soc.* **2005**, *127*, 12890.
[3] [3a] K. Becker, J. M. Lupton, J. Feldmann, S. Setayesh, A. C. Grimsdale, K. Müllen, *J. Am. Chem. Soc.* **2006**, *128*, 680; [3b] J. Jacob, S. Sax, M. Gaal, E. J. W. List, A. C. Grimsdale, K. Müllen, *Macromolecules* **2005**, *38*, 9933.
[4] [4a] D. A. M. Egbe, C. Ulbricht, T. Orgis, B. Carbonnier, T. Kietzke, M. Peip, M. Metzner, M. Gericke, E. Birckner, T. Pakula, D. Neher, U.-W. Grummt, *Chem. Mater.* **2005**, *17*, 6022; [4b] D. A. M. Egbe, B. Carbonnier, E. L. Paul, D. Muehlbacher, T. Kietzke, E. Birckner, D. Neher, U.-W. Grummt, T. Pakula, *Macromolecules* **2005**, *38*, 6269.
[5] [5a] C. J. Tonzola, M. M. Alam, S. A. Jenekhe, *Macromolecules* **2005**, *38*, 9539; [5b] A. P. Kulkarni, Y. Zhu, S. A. Jenekhe, *Macromolecules* **2005**, *38*, 1553.
[6] [6a] J. A. Mikroyannidis, *Syn. Met.* **2005**, *155*, 125; [6b] V. Cimrova, H. Hlidkova, D. Vyprachticky, P. Karastatiris, I. K. Spiliopoulos, J. A. Mikroyannidis, *J. Polym. Sci.: Polym. Phys.* **2006**, *44*, 524.
[7] [7a] F. Wang, M. S. Wilson, R. D. Rauh, P. Schottland, J. R. Reynolds, *Macromolecules* **1999**, *32*, 4272; [7b] F. Wang, M. S. Wilson, R. D. Rauh, P. Schottland, B. C. Thompson, J. R. Reynolds, *Macromolecules* **2000**, *33*, 2083.
[8] [8a] J. Li, Z. Bo, *Macromolecules* **2004**, *37*, 2013; [8b] Z. Fei, B. Li, Z. Bo, R. Lu, *Org. Lett.* **2004**, *6*, 4703; [8c] M. Sun, J. Li, B. Li, Y. Fu, Z. Bo, *Macromolecules* **2005**, *38*, 2651.
[9] J. Chen, H. Peng, C. C. W. Law, Y. Dong, J. W. Y. Lam, I. D. Williams, B. Z. Tang, *Macromolecules* **2003**, *36*, 4319.
[10] T. M. Londergan, Y. You, M. E. Thompson, W. P. Weber, *Macromolecules* **1998**, *31*, 2784.
[11] M. Xu, H. Zhang, L. Pu, *Macromolecules* **2003**, *36*, 2689.
[12] T. Lin, Q. He, F. Bai, L. Dai, *Thin Solid Films* **2000**, *363*, 122.
[13] X. Liu, C. He, X. Hao, L. Tan, Y. Li, K. S. Ong, *Macromolecules* **2004**, *37*, 5965.
[14] G. Kwak, A. Takagi, M. Fujiki, T. Masuda, *Chem. Mater.* **2004**, *16*, 781.
[15] H. Nishide, M. Nambo, M. Miyasaka, *J. Mater. Chem.* **2002**, *12*, 3578.
[16] X. T. Tao, Y. D. Zhang, T. Wada, H. Sasabe, H. Suzuki, T. Watanabe, S. Miyata, *Adv. Mater.* **1998**, *10*, 226.
[17] T. Yamamoto, K. Honda, T. Maruyama, *Syn. Met.* **1997**, *90*, 153.
[18] L. Fomina, R. Salcedo, *Polymer* **1996**, *37*, 1723.
[19] S. F. Swallen, Z. Shi, W. Tan, Z. Xu, J. S. Moore, R. Kopelman, *J. Lumin.* **1998**, *76/77*, 193.
[20] L. Ding, F. E. Karasz, *J. Appl. Phys.* **2004**, *96*, 2272.
[21] R. Jakubiak, L. J. Rothberg, W. Wan, B. R. Hsieh, *Syn. Met.* **1999**, *101*, 230.
[22] R. Gupta, J. Y. Park, V. I. Srdanov, A. J. Heeger, *Syn. Met.* **2002**, *132*, 105.
[23] R. Jakubiak, C. J. Collison, W. Wan, L. J. Rothberg, B. R. Hsieh, *J. Phys. Chem. A* **1999**, *103*, 2394.
[24] N. G. Pschirer, T. Miteva, U. Evans, R. S. Roberts, A. R. Marshall, D. Neher, M. L. Myrick, U. H. F. Bunz, *Chem. Mater.* **2001**, *13*, 2691.
[25] L. Ding, D. A. M. Egbe, F. E. Karasz, *Macromolecules* **2004**, *37*, 6124.

[26] R. Cervini, X. C. Li, G. W. C. Spencer, A. B. Holmes, S. C. Moratti, R. H. Friend, *Syn. Met.* **1997**, *84*, 359.
[27] [27a] Z.-K. Chen, W. Huang, L.-H. Wang, E.-T. Kang, B. J. Chen, C. S. Lee, S. T. Lee, *Macromolecules* **2000**, *33*, 9015; [27b] T. Yasuda, T. Imase, T. Yamamoto, *Macromolecules* **2005**, *38*, 7378; [27c] J. Hou, L. Huo, C. He, C. Yang, Y. Li, *Macromolecules* **2006**, *39*, 594.
[28] A. Dogariu, R. Gupta, A. J. Heeger, H. Wang, *Syn. Met.* **1999**, *100*, 95.
[29] T. M. Brown, J. S. Kim, R. H. Friend, F. Cacialli, R. Daik, W. J. Feast, *Appl. Phys. Lett.* **1999**, *75*, 1679.
[30] V. L. Colvin, M. C. Schlamp, A. P. Alivisatos, *Nature* **1994**, *370*, 354.

